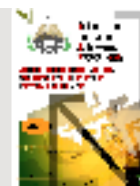




Contents lists available at: <http://qu.edu.iq>

Al-Qadisiyah Journal for Engineering Sciences

Journal homepage: <https://qjes.qu.edu.iq>



Research Paper

Treatment of petroleum refinery wastewater by photo-anodic oxidation process with Gr /Bi-Ni-Sb-SnO₂ rotating photo-anode: Performance and kinetic study

Heba F. Uonis and Ali H. Abbar  

Department of Biochemical Engineering, Al-Khwarizmi College of Engineering, University of Baghdad, Baghdad, 10071, Iraq.

ARTICLE INFO

Article history:

Received 11 September 2025

Received in revised form 28 January 2026

Accepted 15 March 2026

keyword:

Tin oxide

Petroleum waste

Photo-anodic process

Pseudo-first order model

Half-life time

ABSTRACT

This work explores the use of photoelectrocatalysis (PEC) as one of the most advanced oxidation processes (AOPs) for petroleum refinery wastewater (PRW) treatment. A photoelectrochemical reactor equipped with a Gr/Bi-Ni-Sb-SnO₂ photoanode and UVC irradiation was designed to enhance the degradation of pollutants. The effects of key operational parameters, including current density, pH, and anode rotation speed, on the treatment efficiency were systematically evaluated. The results confirmed that increasing the current density provided better chemical oxygen demand (COD) removal, while increasing pH above 5 results in a decrease in COD removal. In addition, increasing the anode rotation speed improved mass transfer and pollutant decomposition up to 200 rpm; after that, no significant improvement was observed, with a slight decrease in COD removal. According to the results, the best performance was achieved at a pH of 5, a current density of 6 mA/cm², and a rotation speed of 200 rpm, achieving a COD removal efficiency of 86.2% in 90 min with an energy consumption of 110.34 kWh/kg⁻¹ COD. Kinetic studies confirmed that the degradation of COD over time exhibited pseudo-first-order kinetics, with an R² of at least 0.999. Considering all factors, the results demonstrate that PEC technology, using Gr/Bi-Ni-Sb-SnO₂ Photoanode, offers a low-energy, sustainable, and facilitating method for the degradation of complex petroleum-derived pollutants. This study highlights the potential of PEC as a practical alternative to conventional industrial wastewater treatment methods.

© 2026 University of Al-Qadisiyah. All rights reserved.

1. Introduction

The wastewater resulting from power or oil production plants is considered one of the heavily polluted waters due to its content of organic compounds, aromatic pollutants, and chemical pollution that comes from dyes, heavy metals, and solvents [1, 2]. Recently, there has been an increase in the demand for oil production and energy production due to the increase in population density and the requirements for energy and oil. This has led to an increase in the number of factories that discharge wastewater significantly each year, threatening human consumption of water and especially aquatic creatures [3, 4]. Through the enactment of laws to protect water and treat wastewater, there has been a development in the treatment of sewage in less energy-consuming ways, instead of traditional chemical processes that are ineffective due to their higher energy consumption. Thus, the trend has shifted towards oxidation in general to reduce energy consumption, as seen in wet oxidation and wet peroxide oxidation [5]. It is well known that the wastewater generated from power generation stations or others is characterized by containing large proportions of pollutants, damage, and negative effects on our health first and the environment second [6]. Ion exchange, flotation, chemical precipitation, and biological systems are traditional methods for eliminating pollution from wastewater. However, a number of disadvantages of these procedures, including their high energy consumption, low removal efficiency, and production of toxic sludge, restrict their widespread use [7, 8]. It has been widely noted that pollutants resistant to biological treatments are often defined by high chemical stability and/or significant challenges in achieving complete mineralization. In these instances, it is imperative to implement reactive systems that are far more efficient than those utilized in traditional purifying methods [9, 10]. Recently, with the advance-

ment of technology, oxidation has also been improved to enhance the treatment process and facilitate the removal of difficult biological or relatively stable chemical pollutants, known as advanced oxidation processes (AOPs) [11, 12]. They work by producing powerful oxidizing agents, such as hydroxyl radicals (OH), which can quickly oxidize a variety of contaminants in a non-selective manner, turning them into CO₂, water, and inorganic species [13, 14]. OH radicals are distinguished by their elevated standard oxidation potential (up to 2.80 V) and their rapid reaction rate relative to conventional oxidants such as chlorine, oxygen, ozone, H₂O₂, or potassium permanganate. As a result, both inorganic and organic solutes can react with OH to produce large rate constants [15]. There are several recognized AOPs, mostly categorized as UV-hydrogen peroxide (UV/H₂O₂), Fenton and photo-Fenton processes, ozone-based methods, photo-catalysis, physical techniques (such as son lysis, microwave and electron beam irradiation), and PEC [16, 17]. The polluting load of waste, which is typically stated as COD, is another factor pertaining to the potential for AOP use. These methods are only appropriate for treating wastes with comparatively low COD levels ≤ 5.0 (g/l), as greater COD concentrations require the use of excessively costly reacting substances. Wet oxidation or incineration are more practical methods for treating wastes with higher concentrations of contaminants [18]. PEC, a very effective kind of AOPs, has been examined as a highly effective method for the removal of recalcitrant organic contaminants [19–21]. Due to PEC sensing's many advantages, including its low background signal, ultra-high sensitivity, low cost, quick analytical time, and simple equipment, numerous researchers have focused on creating semiconductor materials with superior photo electrochemical performance [22, 23]. The photo-anode plays a major role in the collection of charges and the movement of photo-excited electrons from pollution to an external electrical circuit [24].

*Corresponding Author.

E-mail address: ali.abbar@kecbu.uobaghdad.edu.iq; Tel: (+964) 780-328 0891 (Ali Abbar)



Nomenclature

<i>BOD</i>	Biological oxygen demand (<i>ppm</i> or <i>mg/L</i>)
<i>COD</i>	Chemical oxygen demand (<i>ppm</i> or <i>mg/L</i>)
<i>c</i>	Concentration (<i>ppm</i> or <i>mg/L</i>)
<i>E</i>	Voltage of cell (<i>volt</i>)
<i>E_a</i>	Constant anode voltage (<i>volt</i>)
<i>EE</i>	Electrical Energy (<i>kWh</i>)
<i>EEC</i>	Electrical energy consumption (<i>kWh/kg COD</i>)
<i>HLT</i>	Half-life time (<i>min</i>)
<i>I</i>	Current (<i>A</i>)
<i>K</i>	Pseudo-first-order kinetic constant (<i>min⁻¹</i>)

<i>P</i>	Lamp power (<i>kW</i>)
<i>r</i>	Rate of reaction (<i>mg/L.min</i>)
<i>RD</i>	Relative difference (%)
<i>RE</i>	Removal efficiency (%)
<i>t</i>	Time (<i>h</i>)
<i>Subscripts</i>	
<i>i</i>	Initial
<i>f</i>	Final
<i>app</i>	Apparent

In PEC, the material of the anode plays a crucial role in the performance of the process; hence, many photoanodes were developed for treating wastewaters at high efficiency by enhancing the photo-conversion and electron transfer while reducing the combinations between holes and electrons [25–27]. These are nano- TiO_2 [28], $BiVO_4$ -based photo-anodes [29, 30], Ni-PEG-PbO₂/Ti/TiO₂-Ag₂O [31], SnO₂/Mo: BiVO₄, and others [32]. Among them, photo anodes made by SnO₂ doped with bismuth or nickel are the most preferred in PEC due to their low cost, high efficiency, and oxygen overvoltage [33–37]. Yang et al. [33] found that doping SnO₂ anodes with nickel offered excellent properties and can drive both electrocatalysis and photocatalysis for the decomposition of phenol. Domingo-Torner et al. [37] found that Sb-SnO₂ ceramic anodes coated with BiFeO₃ showed high activity in the removal of norfloxacin as a result of the synergistic effect of Bi with SnO₂. Our previous work (Heba and Abbar, 2025), manuscript submitted for publication) showed Gr /Bi-Ni-Sb-SnO₂ (5:5:5:95) photo-anode has good activity for degrading tetracycline due to the combination effect of Ni and Bi on the structure of SnO₂, resulting in the formation of coherent deposits with the best photocatalytic activity. The present work aims to treat PRW by photo-anodic oxidation process using Gr /Bi-Ni-Sb-SnO₂ rotating photo-anode. Although many studies have used PEC for wastewater treatment, none have reported using Gr /Bi-Ni-Sb-SnO₂ for treating petroleum refinery wastewaters. The integration between Ni and Bi with SnO₂ is expected to improve electron mobility, reducing the recombination of electrons and holes generated by UV irradiation, and enhancing the catalytic stability. Applying rotation further improves via increasing mass transfer and light utilization. Accordingly, this study introduces a novel PEC approach that has not previously investigated for real, highly complex wastewater containing recalcitrant organic pollutants such as PRW. The effect of key parameters like current density, pH, and rotation speed on COD removal was investigated by determining the kinetics of degradation.

2. Materials and method

2.1 Characteristics of wastewater

In the present study, fifteen liters of wastewater from Al-Dora petroleum refinery in Iraq were obtained from the physical treatment unit's feeding collecting tank in the plant and stored at 4 °C until needed. The characteristics of treated effluent and untreated wastewater are shown in Table 1 according to the physical unit that the plant management gave.

Table 1. Characteristics of Al-Dora refinery plant wastewater.

Characteristic	Input	Output
Temperature, °C	32.00	28.00
pH	07.30	07.30
Turbidity, (NTU)	75.40	21.30
TDS, (mg/L)	938.0	1066.0
COD, (mg/L)	435.00	68.00
BOD, (mg/L)	176.00	16.00
Oil, (mg/L)	163.10	05.50
SO ₄ ²⁻ , (mg/L)	340.00	380.00
Cl ⁻ , (mg/L)	636.00	536.00
PO ₄ , (mg/L)	00.93	00.65

2.2 Materials and chemicals

SnCl₂.2H₂O, SbCl₃, Na₂SO₄, NiCl₂, BiCl₃, Isopropyl alcohol (IPA), 1,4-benzoquinone(p-BQ), ammonium oxalate monohydrate (AO), H₂SO₄, NaOH and citric acid were purchased from Merck. Analytical grade compounds were all utilized without additional purification. Every solution was made with deionized water.

2.3 Preparation of Gr /Bi-Ni-Sb-SnO₂ photo-anode

Gr /Bi-Ni-Sb-SnO₂ photo-anode was prepared according to a similar procedure mentioned in our previous work [38]. A graphite rod having a diameter of 20mm and a length of 50 mm was activated by soaking in a boiled water for 1h than, followed by putting in an electrochemical cell containing 1.44M sulfuric acid electrolyte in which the graphite rod act as anode and hollow cylinder graphite as cathode where current was applied at 14 mA/cm² for 30 min. The activated graphite rod was then used as a cathode in an electrochemical cell used to electrodeposit tin and other elements from their salts. In this case, an electrolytic solution containing the following composition was used: 67.5 (g/L) SnCl₂2H₂O, 2.25 (g/L) SbCl₃, 3.56 (g/L) NiCl₂, 4.73 (g/L) BiCl₃, and 57.5 (g/L) citric acid. A current density of 10 mA/cm² was applied for 1h at 50 °C and 250 rpm as rotation for the cathode. The electroplated graphite was then rinsed in distilled water several times and dried at 100 °C for 1h followed by calcinating at 500 °C for 3h. the above procedure resulted in a photoanode called Gr /Bi-Ni-Sb-SnO₂ (5:5:5:95) based on the constituents of the plating solution.

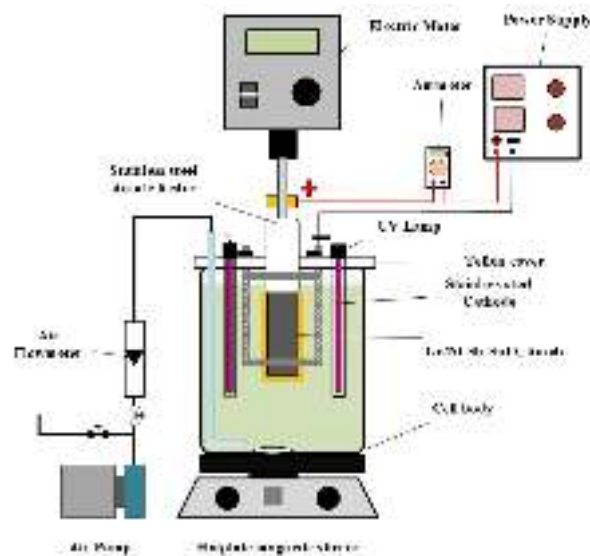


Figure 1. Photo-anodic oxidation system

2.4 Photo electrochemical system

The PEC system is composed of an electrochemical cell, an overhead electric motor (PHOEN RSO: 20D), an air compressor type-HAILEA/aco-280, a magnetic hot plate (ISO LAP), and a power supply type-UNI-T/UTP-3315TFL. The required current was monitored ammeter UNI-UT90A. While the flow rate of air was adjusted at 1 L/min via a control valve connected to an air flow meter, which has a range of 0.5-5 L/min. The PEC system is schematically depicted in Fig. 1. The photo-electro reactor was a Perspex cylindrical reactor that was 10 cm in diameter and 19.5 cm in length. A Perspex covering with an external diameter of 12 cm and a thickness of 1 cm was included. The cover had three holes drilled in it. The first is situated in the center and has a diameter of 2.5 cm for inclusion of the anode. The others are situated 2.5 from the center and have the same diameter (2 cm) for inclusion of two UVC lamps (Starlight R-CAN, Texas, USA, 10W, and λ of 253.7 nm). Based on López-Peñalver's work [39], UVC was chosen for this study. They discovered that utilizing UV with $\lambda = 254$ nm produced the optimum photo degradation of TC. UVC was used as a cause of irritation in other investigations as well [40]. The cathode

was a hollow stainless steel cylinder that measured 3.8 cm in diameter and 1 mm in thickness. It had holes evenly spaced over its lateral surface, each measuring 5 mm in diameter. The cathode was secured to the cover by two 5 mm diameter holes. The anode was composed of two sections, the first is a stainless steel current feeder measuring 0.7 cm in diameter and 17 cm in length, bounded by a Teflon shield at its lower section (9 cm) to prevent it from the corrosion while the second section is Gr/Bi-Ni-Sb-SnO₂ photo-anode. A copper ring that was placed around the anode feeder and connected to the power supply's positive pole allowed for the anode's electrical connection. The photoanodic oxidation was performed at room temperature. Firstly, 750 ml of wastewater was taken and put in a 1L beaker over a hotplate with magnetic stirrer, then Na₂SO₄ was added to make a concentration of 0.05M as a support electrolyte then allowed the mixture to homogenize under stirring for 15 min. After that, the solution was transferred to the cell, with supplying air to the solution for a further 15 min with switching on the UV lamps. The required current with a suitable current density was applied for a period of 90 min. Every 15 min sample was taken to measure its COD value.

2.5 Characterization and performance

The morphology of the photo-anode was identified by the SEM technique using SEM (FEI Company, Netherlands) operated at HV = 25 kV, spot = 8.0, bias = 1400 V. The crystalline structure of the photo-anode was recognized by X-ray diffractometer (XRD 6000/Shimadzu/Japan) with CuK α radiation of 1.5405 Å and operated at 40 kV, 30 mA, step size of 0.2°, and scan step time of 1.2s. The testing was performed in the range of 2 θ between 20 and 80°. COD was determined by digesting the sample with potassium permanganate at 150°C for 2h using a thermo reactor (RD125, Lovibond). The sample was allowed to cool, and its COD value was obtained by putting the digested sample in a spectrophotometer (MD200, Lovibond). The oil content was measured by HORIBA OCMA-350, while turbidity was measured using Lovibond TurbDirect /serial number12/1805. Cl- concentration was determined by Photo Flex Series (WTW model no 14541, Germany). The removal efficiency(RE%) of COD was evaluated by Eq. 1 [41].

$$RE (\%) = \frac{COD_i - COD_f}{COD_i} \times 100 \quad (1)$$

RE (%) stands for the COD removal efficiency, COD_i for the initial COD (mg/L), and COD_f for the final COD (mg/L) in the computation. The total amount of energy necessary to digest one kilogram of COD is known as EEC. EEC (kWh/kg COD) can be calculated using Eqs. 2 and 3 [41].

$$EEC = \frac{EE_{total} \times 1000}{COD_i - COD_f} \times v \quad (2)$$

$$EE_{total} = (P + E \times I) \times t \quad (3)$$

In this case, P is lamp power in watts, I stands for current in amperes, E for applied cell potential in volts, and t for electrolysis period (hour). Phenol concentration was identified using Hach Company/Hach Lange GmbH, USA's Method 8047, whereas chloride ion concentration was measured using the Photo Flex Series (WTW, model number 14541, Germany). Multiple replications were performed for each run, and the mean value in this study was taken after verifying the accuracy of the experimental results by assessing the relative difference (RD) using Eq. 4, which must be less than 10% [42]:

$$RD = \frac{(C_1 - C_2) \times 100\%}{(C_1 + C_2)/2} \quad (4)$$

3. Results and discussion

3.1 Characterization of photoanode

Figure 2 shows XRD results for Gr/Bi-Ni-Sb-SnO₂(5:5:5:95) where strong peaks for tetragonal rutile SnO₂ were observed at 2 θ = 26.45°(110), 33.85°(101), 37.95°(200), 51.65°(211), 54.45°(220), 59.55°(002), 61.85°(310), 64.55°(112), and 65.85°(301) (PDF no. 41-1445) [43]. Furthermore, strong peaks were observed at 2 θ =28.4°, 30.1°, 34.6 and 48.7 corresponding to Sb₂O₅ [44–46]. Peaks at 2 θ = 26.45°(002), 42.4°(111), 44.5°(101), 54.45°(004) and 77.4°(006) are belong to graphite [47]. Peaks of α -Bi₂O₃ were observed at 2 θ =(27.4°(120), 33.3°(200), 46.3°(041)) which belong to monoclinic Bi₂O₃ crystal structure (JCPDS Card No.01-072-0398) [48, 49]. Peaks at 2 θ =37.20°(111), 43.095°(200), 62.86°(220), and 75.20°(311) were observed, which corresponds to the cubic NiO crystal structure (JCPDS Card No: 78-0643) [50–52]. Furthermore, a single peak at 2 θ = 56.3° was observed,

which corresponds to Ni₂O₃ [53]. The results of XRD confirm the successful doping of Bi and Ni within the structure of SnO₂ forming Gr/Bi-Ni-Sb-SnO₂ photoanode. Figure 3 shows the SEM of Gr/Bi-Ni-Sb-SnO₂ (5:5:5:95) photoanode at two magnifications (1000 \times and 2000 \times). Adding Ni and Bi resulted in a pale yellow structure proposing successful formation of the composite NiO and Bi₂O₃ [49, 52]. The shape of the deposits turns sharp edges aggregates. No cracks were detected, which could result in an improvement in the stability and lifespan of the electrode [54]. Figure 4 shows the EDS of Gr/Bi-Ni-Sb-SnO₂ (5:5:5:95) anode, which confirms the existence of O, Sn, Sb, Bi, and Ni within the structure of film deposited on Gr. Oxygen evolution potential (OEP) is one of the most important parameters that gives an indication of the catalytic activity of an anode, where higher values represent the best catalytic activity in which few side reactions could be happened with OH generation [55].

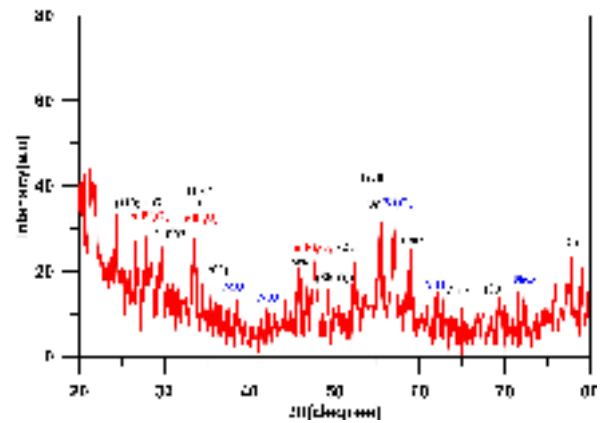


Figure 2. XRD for Gr/Bi-Ni-Sb-SnO₂ (5:5:5:95) photo anode

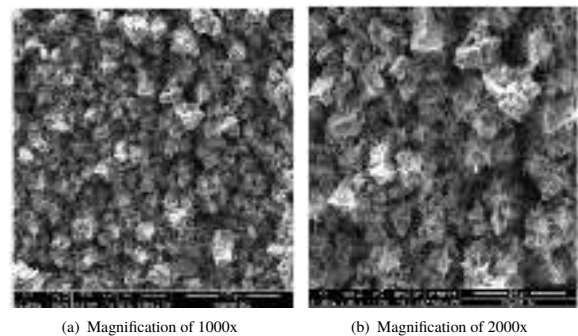


Figure 3. SEM of Gr/Bi-Ni-Sb-SnO₂ (5:5:5:95).

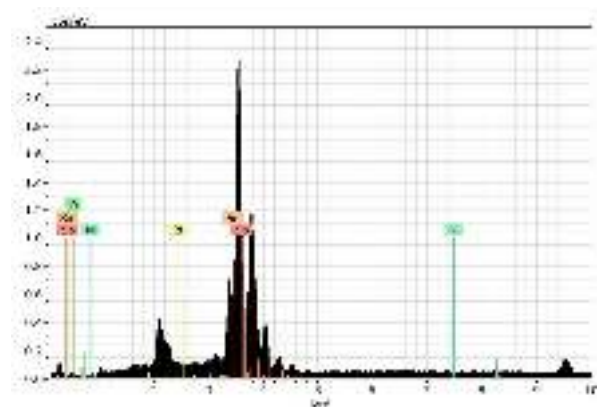


Figure 4. EDS for Gr/Bi-Ni-Sb-SnO₂ (5:5:5:95) anode

Figure 5 displays LSV for Gr/Bi-Ni-Sb-SnO₂ (5:5:5:95) anode compared with no doping case (Gr/Sb-SnO₂) in sodium sulfate solution (0.1 M) at a scan rate

of 10 mVs^{-1} . Results confirmed the present photoanode has good catalytic activity with OEP of 2.14 V (vs. Ag/AgCl), which is higher than SnO_2 alone and other related SnO_2 anodes prepared by thermal decomposition methods [56,57]. Furthermore, the present photoanode could be considered cheap in comparison with the expensive boron-doped diamond anode, non-toxic in comparison with the PbO_2 anode, and easy to scale-up [58].

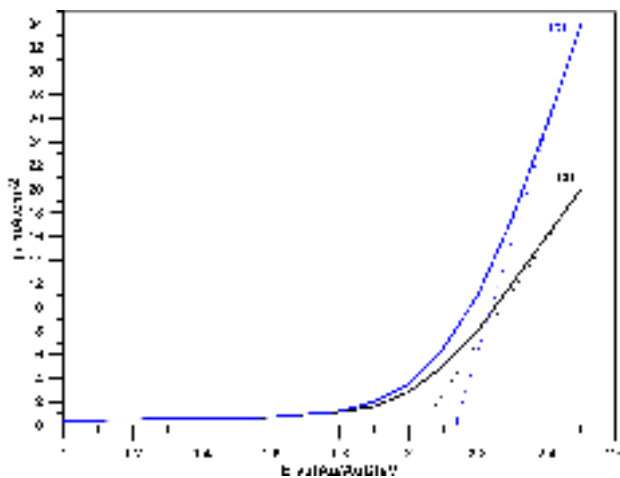


Figure 5. LSV for Gr/ Bi-Ni-Sb-SnO2 (5:5:5:95)(a) compared with Gr/ Sb-SnO2 anode(b).

3.2 Effect of operating variables

3.2.1 Effect of current density

In PEC, current density plays a vital role in the performance of oxidation in this process [59]. Figure 6 shows the impact of current density on the COD removal efficiency at different values under an initial pH of 5 and a rotation speed of 200 rpm. It was observed that the RE% increases with increasing current density up to 6 mA/cm^2 beyond which a decrease in RE% occurs.

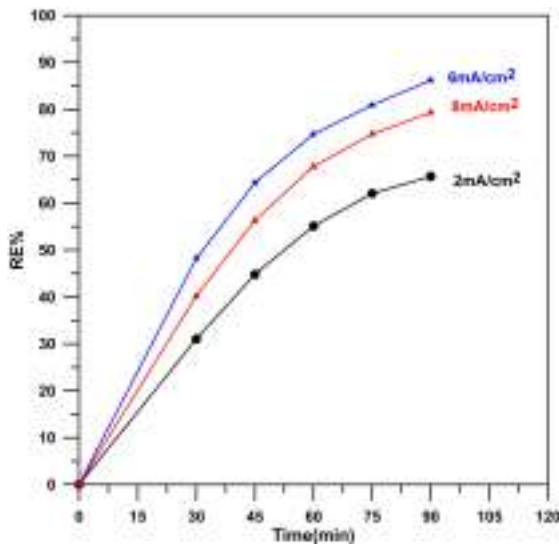


Figure 6. Impact of current density on RE%. pH=5, 200 rpm.

Consequently, a current density of 6 mA/cm^2 is recommended. The increase in COD removal with increasing current density up to 6 mA/cm^2 can be explained as more hydroxyl radicals are generated with increasing current. Moreover, increasing the current can cause a decrease in the recombination rate of electrons and holes generated by UV irradiation, and thus, more radicals are generated on the photoanode [60]. With increasing current density, a large number of oxygen bubbles are formed, which results in a loss of current towards O_2 evolution rather than OH radicals generation [61]. Ahdour et al. [62] found a similar behavior in the degradation of tetracycline using $\text{BaHPO}_4/\text{SSA}$ photoanode, where the optimum current density was 10.56 mA/cm^2 within a range of $4\text{--}12 \text{ mA/cm}^2$. Orimolade et al. [63] found a similar effect of current

density in the degradation of paracetamol using a FTO- $\text{BiVO}_4/\text{BiOI}$ photoanode, where the degradation rate increased with increasing current density from 5 to 15 mA/cm^2 and then decreased at 20 mA/cm^2 . Similar behaviors have been reported by other works using different photoanodes and contaminants [35,47,64]. In support of our results, most previous studies have confirmed the existence of an optimum value of current density or voltage that achieved maximum generation of OH and thus the highest degradation rate, beyond which no improvement or decrease in the removal rate occurs because OH is no longer dominant [59,65,66]. Furthermore, the improvement in the performance of the present photoanode could be linked to the effect of N_i and B_i addition. Pirsahab et al. [67] found that excellent humic acid removal occurred when using $\text{NiTiO}_2\text{-NT}$ photoanode due to the presence of N_i , which narrows the band gap leading to enhanced electron transfer rate and reduced recombination of electrons and holes.

3.2.2 Effect of pH

The pH of the solution plays a fundamental role in the oxidation mechanism during PEC and thus affects the degradation rate of contaminants. pH influences the formation of reactive species such as OH, the formation rate of which increases under acidic conditions [68]. pH also affects the surface charge of the photoanode, its stability, and corrosion phenomena [69]. Furthermore, pH affects the band bending of the semiconductors that make up the photoanode, as high band bending can occur on the semiconductor surface under acidic conditions due to the adsorption of more organic contaminants, thus increasing the oxidation process, and vice versa under alkaline conditions [61,70]. Figure 7 shows the effect of pH on the COD removal rate in terms of RE% under 6 mA/cm^2 and 200 rpm. It can be seen that the COD removal is almost constant with a slight increase as the pH moves from 3 to 5, reaching 86.2%. However, it starts to decrease with further increase in pH and reaches 74.7% at pH 9. Zhou et al. [71] found that pH 2 is more favorable for the degradation of landfill leachate by PEC using TiO_2/Ti photoanode than alkaline conditions. Umukoro et al. [64] found that the best ciprofloxacin removal occurred at pH 5.4 and decreased when pH became 4 or 8 using PEC with $\text{MoS}_2\text{-SnO}_2/\text{EG}$ nanocomposite photoanode. Similar results were found in previous works [72,73]. However, operation at neutral conditions also yielded good COD removal of 81.6% at a COD level of 80 mg/L below the standard limit for discharge of PRW to the environment. These results confirmed the good activity of the Gr/Bi-Ni-Sb-SnO₂ photoanode in treating one of the most hazardous wastewaters generated by industry.

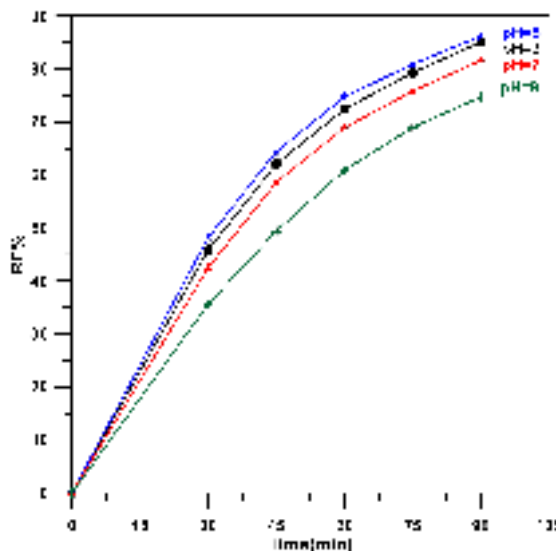


Figure 7. Impact of pH on RE% . 6 mA/cm^2 , 200 rpm.

3.2.3 Effect of anodic rotation speed

Rotation speed is an essential operating parameter in PEC used for wastewater treatment. It has a direct impact on mass transfer, hydrodynamics, and light utilization efficiency. The photoanode's rotational motion (as in a spinning disc or rotating electrode system) improves the diffusion of pollutants and dissolved oxygen towards the photoactive surface by decreasing the thickness of the boundary layer around the photoanode [26]. Light penetration and effective charge separation at the photo anode surface are enhanced by increasing turbulence at the electrode-solution interface caused by an increase in the rotation speed

[74]. High speed prevents deactivation of the photo anode and reduces fouling [75]. Figure 8 illustrates the effect of photoanode rotation speed on the removal rate of COD under 6 mA/cm^2 and $\text{pH}=5$. It can be seen that increasing rotation speed up to 200 rpm gives higher removal of COD, while further increase in rotation speed has no significant effect on COD removal and causes a slight decrease in RE% due to the effect of turbulence and mechanical stress resulting from vibration of the anode that could cause destabilizing the intermediates [26]. Similar results were found by Cho et al. [74] in the removal of methylene blue using rotating TiO_2 nanotubes photo anode. The rotation speed of 90 rpm is the best in the removal of methylene blue, while a higher speed resulted in a decrease in methylene blue removal. Xu et al. [76] found that a rotation speed of 90 rpm is the best for the removal of Rhodamine B using TiO_2 rotating disk photoanode.

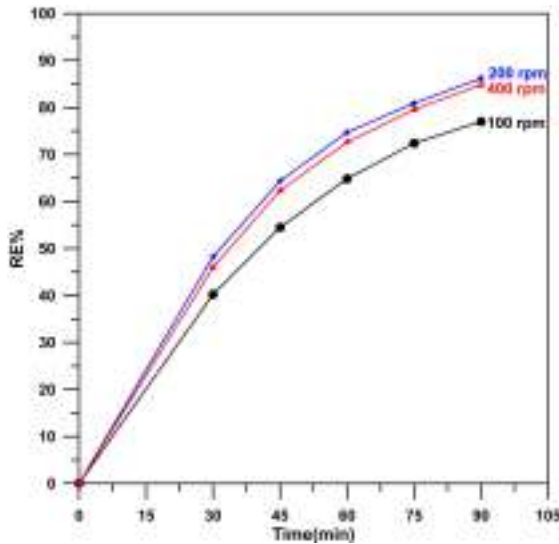


Figure 8. Impact of rotation speed on RE%. 6 mA/cm^2 , $\text{pH}=5$

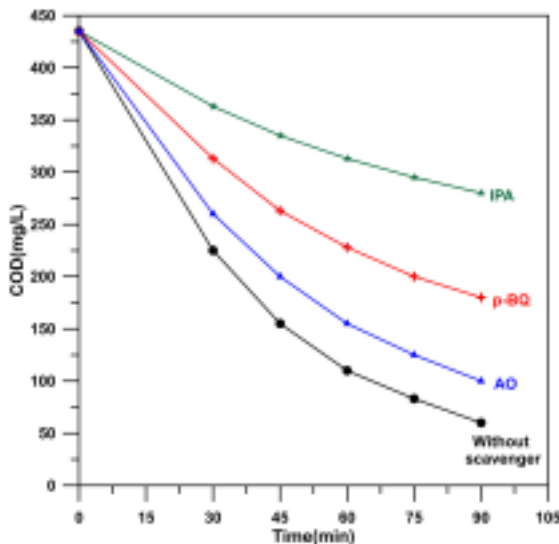


Figure 9. Effect of various scavengers on the COD removal by PEC process. 6 mA/cm^2 , $\text{pH}=5$, 200rpm.

3.3 Free Radical Recognition

To determine the role of free radicals (OH , O_2^- , and h^+) that can be generated in PEC, three known scavengers (IPA, p-BQ, and AO) were used at a concentration of 5 mM [38]. They were added to a PEC operating at 6 mA/cm^2 , $\text{pH} 5$, and 200 rpm, as shown in Fig. 9. It was observed that COD degradation was suppressed upon the addition of the scavengers. The addition of IPA resulted in a decrease in RE% from 86.2% to 35.6%, confirming that OH is the dominant radical in COD degradation. The addition of p-BQ resulted in a decrease in RE% to 58.6%, confirming an important role for O_2^- during PEC, which

shares its effect with OH. h^+ has a minor effect on COD removal. Ahdor et al. [62] reported that O_2^- is the major radical in the PEC of tetracycline using the $\text{BaHPO}_4/\text{SSA}$ photoanode, with a minor role for OH and h^+ . Kang and Kim [32] reported similar behavior during the PEC treatment of tetracycline hydrochloride using the $\text{SnO}_2/\text{Mo:BiVO}_4$ photoanode. The discrepancy with other work may be due to the catalytic activity of the photoanode used in the degradation process.

3.4 Reusability of PEC

From an industrial application perspective, the long-term efficiency and stability of PECs are key factors in evaluating their performance. In this study, the stability of the photoanode in a PEC was verified by sequentially running the system through multiple cycles. In each cycle, the anode was cleaned with distilled water and ethanol and then used in the next cycle. Figure 10 shows the RE% at different cycles operated at 6 mA/cm^2 , $\text{pH} 5$, and 200 rpm. A decrease in RE% was observed from 86.2% to 75.5% after 5 cycles, confirming the photoanode's effectiveness in removing COD from PRW.

3.5 Kinetic studies

Studying PEC kinetics has several benefits including determining the optimal PEC based on high removal efficiency with low energy consumption, providing insight into the rate of contaminant oxidation, providing a basis for calculating reactor size, operating time and electrode surface area when scaling up to industrial scale, and preventing overtreatment by stopping the process at the point of diminishing returns [77]. For PEC process, the degradation rate of COD can be fitted to a pseudo-first order kinetic model as follows Eq. 5 [64, 78, 79]:

$$r = \frac{d\text{COD}}{dt} = k_{app} \text{COD} \quad (5)$$

where k_{app} represents a pseudo-first-order kinetic constant.

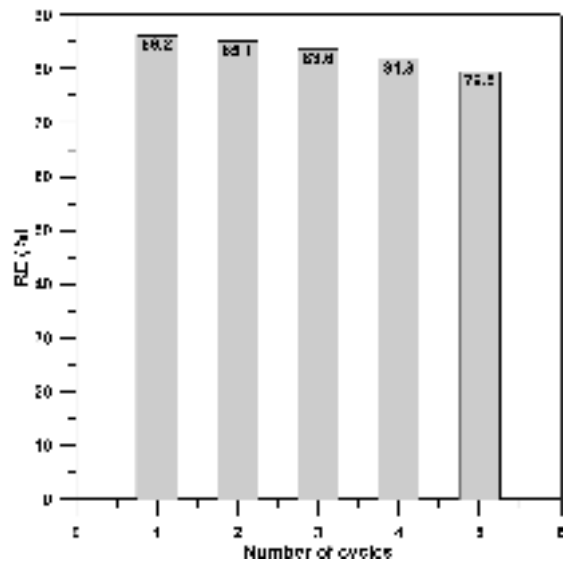


Figure 10. Reusability of Gr/ Bi-Ni-Sb-SnO2 (5:5:5:95) photo-anode.

The integration of Eq. 5 subject to the initial conditions $\text{COD}=\text{COD}_i$ at $t=0$ leads to the following Eq. 6:

$$\ln \frac{\text{COD}}{\text{COD}_i} = k_{app} t \quad (6)$$

Figures 11, 12, and 13 illustrate the COD degradation over time for different operating variables with the relevant plot of $\ln(\text{COD}/\text{COD}_i)$ versus time. Table 2 shows the k_{app} values with the respective R^2 and the half-life time (HLT) calculated as $(\ln(2)/k_{app})$. It can be seen that all decays of COD with time follow pseudo-order behaviour, driven by OH attack on aromatic contaminants, which is consistent with most works in PEC. Furthermore, current density has the greatest influence on k_{app} than other variables, confirming that the current controls the oxidation rate. It is observed that k_{app} increases with increasing current density up to an optimum value after which it starts to decrease with increasing current Table 2.

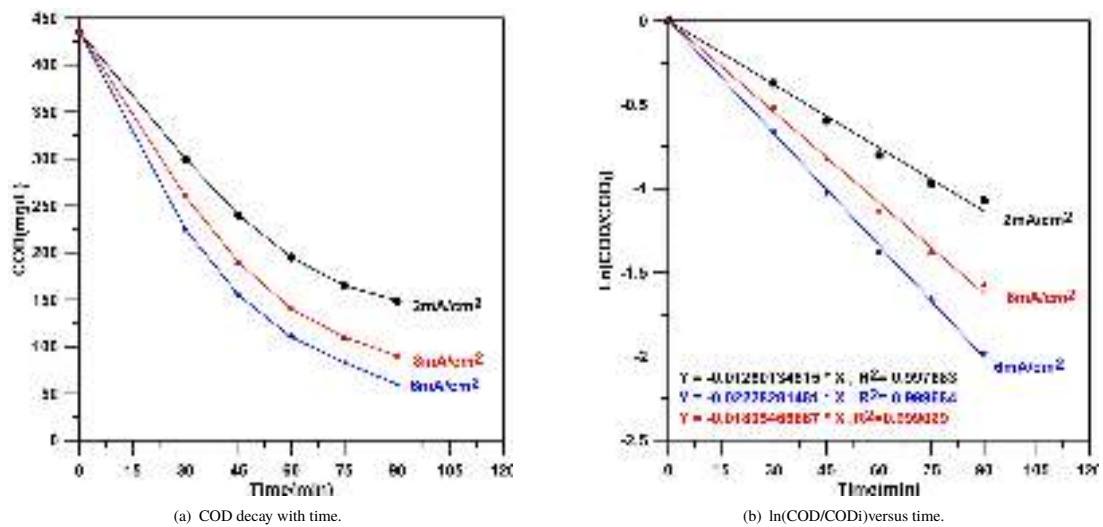


Figure 11. kinetic results for effect of current density.

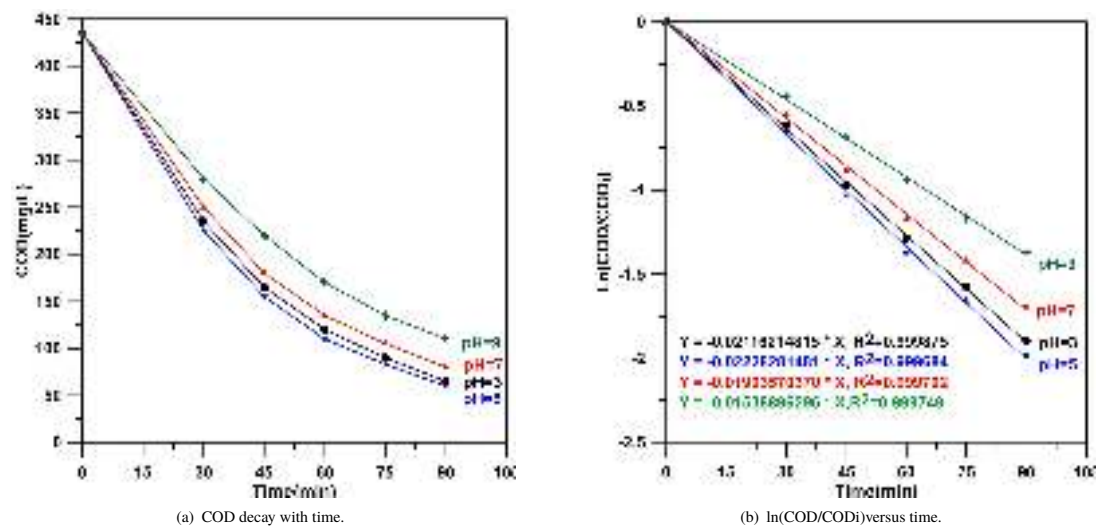


Figure 12. kinetic results for effect of pH.

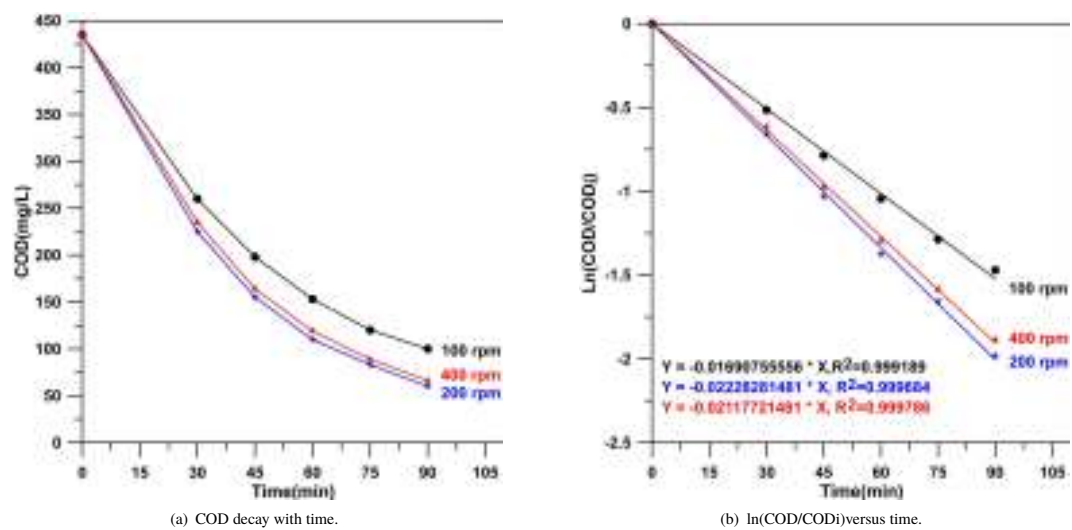


Figure 13. kinetic results for effect of rotation speed.

Table 2. Pseudo-first order rate constant at different operating variables.

Operating variables		K_{app}	R^2	HLT	RE	EEC
Parameter	Value	(min^{-1})		(min)	(%)	(kWh/kg)
Current density (mA/cm^2)	2	0.0126	0.997683	55.01	65.7	1.302
	6	0.0223	0.999684	31.08	86.2	3.648
	8	0.0181	0.999029	38.29	79.31	6.08
pH	3	0.0212	0.999875	32.69	85.05	3.406
	5	0.0223	0.999684	31.08	86.2	3.648
	7	0.0190	0.999702	36.48	81.6	3.854
	9	0.0154	0.999749	45.01	74.7	4.321
Rotation (rpm)	100	0.0169	0.999189	41.01	77	4.18
	200	0.0223	0.999684	31.08	86.2	3.648
	400	0.0212	0.999786	32.69	84.827	3.415

A similar observation was made by Brillas et al. [80] in their work on the degradation of dyes by PEC. The lowest HLT value of about 31 (*min*) is achieved at 6 mA/cm^2 , pH 5, and 200 rpm, which is within the general range in PEC systems (3-70 *min*) depending on the type of pollutants, light source (solar or UV), photoanode material and current density [81]. Table 3 shows the characteristics of the wastewater after treatment. It can be seen that in addition to removing COD and reducing its value to 60 (mg/L), TDS was also reduced by 28.57%, BOD was lowered to below the standard limit (40 mg/L), and turbidity was significantly reduced by 92.9%, as was oil content (97.85%). SO_4^{2-} increased due to the use of a supporting electrolyte, while Cl^- decreased due to the indirect oxidation of Cl^- to Cl_2 at the anode surface, which reacts with water to form ClO^- , which attacks organic compounds and converts them to CO_2 and H_2O . Therefore, the chlorine ions present in the PEC process have other advantages.

Table 4. PEC applied to different types of pollutants in comparison with present work.

Photo anode / Fabrication method	Cathode	Pollutant	Operational conditions	RE%	Ref.
Gr/Bi-Ni-Sb-SnO ₂ Electrochemical deposition	SS	PRW	6 mA/cm^2 , pH=5, time=90 min, UVC(20W)	86.2	This work
TiO ₂ /BDD Sol-gel/Spin-coating	Graphite	Glyphosate	3 mA/cm^2 , pH=4, time=300 min, UVC(9W)	99.5	[59]
TiO ₂ /BDD Electrophoretic Deposition	Platinum	Diclofenac	2.2 mA/cm^2 , pH=5.5, time=120 min, UVC(25W)	98.5	[82]
N-rGO-TiO ₂ /SS Sol-gel method/dip-coating	SS	Phenol	Ea=0.8V, pH=1, time=180 min, UV-VIS (150 W)	45.0	[83]
FTO/BiVO ₄ /BiOI Electrochemical deposition	Platinum	Paracetamol	Ea=1.5V, pH=5.9, time=120 min, UV-VIS (100 W)	68.0	[84]
Sn ₃ O ₄ /TiO ₂ /Ti Spin-coating	DSA	Azo acid yellow 17	Ea=0.5V, pH=2.0, time=60 min, UV-VIS (125 W)	95.0	[85]
Ti/TiO ₂ (NT) Electrochemical anodization	Graphite	Real oil-produced water	Ea=2.5 V, time=120 min, UVC(36W)	73.0	[86]
TiO ₂ /Ti sol-gel	Titanium	Oil Field wastewater	Ea=30V, pH=2.0, time=240 min, UVC(50 W)	47.4	[87]
BiVO ₄ /FTO Electrochemical deposition	Hemin / Cu Carbon felt	Tetracycline	Ea=0.8V, pH=5.9, time=120 min, xenon lamp	60.6	[88]

4. Conclusion

The results of this study demonstrate that the PEC system is an efficient and environmentally friendly technology for treating industrial wastewater from petroleum refineries. RE% was found to be strongly influenced by three operating factors: current density, pH, and anodic rotation speed. The best results were obtained at a current density of 6 mA/cm^2 , pH 5, and a rotation speed of 200 rpm, where an RE% of 86.2% was achieved. The anode rotation speed plays a significant role in the degradation efficiency due to improved mass transfer; however, very high speeds have a minimal effect and are associated with increased energy consumption. The kinetic study showed that COD followed a pseudo-first-order model for all parameter conditions, indicating that the degradation rate depends on the COD concentration, while the concentration of the reactive reagents is assumed to be constant during PEC. The scavengers test revealed that OH is the dominant radical in COD degradation, indicating that the oxidation process is controlled by OH. The Gr/Bi-Ni-Sb-SnO₂ photoanode demonstrated excellent reusability after five cycles, indicating its robust structural stability and resistance to deactivation. The adoption of concentric configuration of the electrode with rotation of anode makes the present system more feasible to scale-up as the rotation effect improves current and voltage distribution uniformly with ensuring good light absorption with minimal fouling. Overall, this study demonstrates that PEC technology, utilizing advanced photoanodes such as Gr/Bi-Ni-Sb-SnO₂, effectively removes organic and petroleum pollutants with lower energy consumption and a reduced negative environmental impact. Therefore, this technology can be considered a promising approach for industrial wastewater treatment and promoting more

Table 3. Characteristics of the treated wastewater.

Characteristic	Initial	Final(after treatment)
pH	07.30	05.00
Turbidity, (NTU)	75.40	05.34
TDS, (mg/L)	938.0	670
COD, (mg/L)	435.00	60.00
BOD, (mg/L)	176.00	26.00
Oil, (mg/L)	163.10	03.50
SO_4^{2-} , (mg/L)	340.00	680.0
Cl^- , (mg/L)	636.00	336.00

3.6 Comparison with related works

Table 4 shows a comparison between the present work and other related works on PEC using different photoanodes and various pollutants. Most of these works focus on the removal of a single pollutant, and a few on real wastewater using either constant current density or constant anode voltage (Ea). Based on previous works, the present work yields better results in terms of pollutant removal from complex wastewater (PRW) in a short time, with low lamp power, and easy photoanode fabrication. Furthermore, to estimate the electrical energy consumption in the present work, the system was operated under optimal conditions (6 mA/cm^2 , pH = 3, and 200 rpm) with a constant current of 0.18 A applied for 90 minutes, while the cell voltage was recorded in the range of 3.6–4.0 V. The calculated EEC was 110.34 kWh/kg COD, which is relatively low compared to those reported in previous studies using PEC, where the power consumption range was limited to 30–300 kWh/kg COD [81], making the present work more feasible for industrial applications. It is important to note that the application of rotation leads to a lower applied voltage required for PEC and thus lower energy consumption.

sustainable water resource management.

Authors' contribution

All authors contributed equally to the preparation of this article.

Declaration of competing interest

The authors declare no conflicts of interest.

Funding source

This study didn't receive any specific funds.

Data availability

The data that support the findings of this study are available from the corresponding author upon reasonable request.

Acknowledgements

Authors would like to express their grateful for the biochemical Engineering Department staff at the University of Baghdad, Baghdad, Iraq, for their helpful and technical support.

REFERENCES

- [1] Z. Abbas and A. Abbas, "Optimization of the electro-fenton process for cod reduction from refinery wastewater," *Environmental Engineering Management Journal (EEMJ)*, vol. 19, no. 11, pp. 2029–2037, 2020. [Online]. Available: <https://doi.org/10.30638/eemj.2020.192>

- [2] A. Srinivasan and T. Viraraghavan, "Decolorization of dye wastewaters by biosorbents: a review," *Journal of environmental management*, vol. 91, no. 10, pp. 1915–1929, 2010. [Online]. Available: <https://doi.org/10.1016/j.jenvman.2010.05.003>
- [3] L. Da Silva, R. Ruggiero, P. Gontijo, R. Pinto, B. Royer, E. Lima, and T. Calvete, "Adsorption of brilliant red 2be dye from water solutions by a chemically modified sugarcane bagasse lignin," *Chemical Engineering Journal*, vol. 168, no. 2, pp. 620–628, 2011. [Online]. Available: <https://doi.org/10.1016/j.cej.2011.01.040>
- [4] M. Jiad and A. Abbar, "Treatment of petroleum refinery wastewater by electro-fenton process using a low-cost porous graphite air-diffusion cathode with a novel design," *Chemical Engineering Research and Design*, vol. 193, pp. 207–221, 2023. [Online]. Available: <https://doi.org/10.1016/j.cherd.2023.03.021>
- [5] K. Pirkanniemi and M. Sillanpaa, "Heterogeneous water phase catalysis as an environmental application: a review," *Chemosphere*, vol. 48, no. 10, pp. 1047–1060, 2002. [Online]. Available: [https://doi.org/10.1016/S0045-6535\(02\)00168-6](https://doi.org/10.1016/S0045-6535(02)00168-6)
- [6] O. Abdelwahab, N. Amin, and E. El-Ashtouky, "Electrochemical removal of phenol from oil refinery wastewater," *Journal of hazardous materials*, vol. 163, no. 2-3, pp. 711–716, 2009. [Online]. Available: <https://doi.org/10.1016/j.jhazmat.2008.07.016>
- [7] H. Eccles, "Treatment of metal-contaminated wastes: why select a biological process?" *Trends In Biotechnology*, vol. 17, no. 12, pp. 462–465, 1999. [Online]. Available: [https://doi.org/10.1016/S0167-7799\(99\)01381-5](https://doi.org/10.1016/S0167-7799(99)01381-5)
- [8] M. Jiad, A. Abbar, and Z. Jabbar, "Advanced treatment of petroleum refinery wastewater by electro-fenton and photo-catalytic processes," *environmental technology reviews*, vol. 14, no. 1, pp. 400–426, 2025. [Online]. Available: <https://doi.org/10.1080/21622515.2025.2479713>
- [9] P. Fedorak and S. Hrudey, "The effects of phenol and some alkyl phenolics on batch anaerobic methanogenesis," *water research*, vol. 18, no. 3, pp. 361–367, 1984. [Online]. Available: [https://doi.org/10.1016/0043-1354\(84\)90113-1](https://doi.org/10.1016/0043-1354(84)90113-1)
- [10] R. Barreiro and J. Pratt, "Toxic effects of chemicals on microorganisms," *water environment research*, vol. 64, no. 4, pp. 632–641, 1992. [Online]. Available: <https://doi.org/10.1002/j.1554-7531.1992.tb00045.x>
- [11] W. Elmobarak, B. Hameed, F. Almomani, and A. Z. Abdullah, "A review on the treatment of petroleum refinery wastewater using advanced oxidation processes," *Catalysts*, vol. 11, no. 7, p. 782, 2021. [Online]. Available: <https://doi.org/10.3390/catal11070782>
- [12] A. Biń and S. Sobera-Madej, "Comparison of the advanced oxidation processes (uv, uv/h₂o₂ and o₃) for the removal of antibiotic substances during wastewater treatment," *ozone: science engineering*, vol. 34, no. 2, pp. 136–139, 2012. [Online]. Available: <https://doi.org/10.1080/01919512.2012.650130>
- [13] S. Yu, Z. Xie, X. Wu, Y. Zheng, Y. Shi, Z. Xiong, and B. Lai, "Review of advanced oxidation processes for treating hospital sewage to achieve decontamination and disinfection," *chinese chemical letters*, vol. 35, no. 1, p. 108714, 2024. [Online]. Available: <https://doi.org/10.1016/j.ccl.2023.108714>
- [14] A. Thakur, r. Kumar, A. Kumar, r. Shankar, n. Khan, K. Gupta, and R. Arya, "Pharmaceutical wastewater treatment via advanced oxidation-based integrated processes: an engineering and economic perspective," *Journal of Water Process Engineering*, vol. 54, no. 1, p. 103977, 2023. [Online]. Available: <https://doi.org/10.1016/j.jwpe.2023.103977>
- [15] p. Bautista, A. Mohedano, J. Casas, J. Zazo, and J. Rodríguez, "An overview of the application of fenton oxidation to industrial wastewater treatment," *Journal of chemical technology biotechnology*, vol. 83, no. 10, pp. 1323–1338, 2008. [Online]. Available: <https://doi.org/10.1002/jctb.1988>
- [16] P. Pandis, C. Kalogirou, E. Kanellou, c. Vaitis, M. Savvidou, G. Sourkouni, and C. Argiris, "Key points of advanced oxidation processes (aops) for wastewater, organic pollutants and pharmaceutical waste treatment: a mini review," *ChemEngineering*, vol. 6, no. 1, p. 8, 2022. [Online]. Available: <https://doi.org/10.3390/chemengineering6010008>
- [17] N. Roslan, H. Lau, N. Suhaimi, N. Shahri, S. Verinda, M. Nur, and A. Usman, "Recent advances in advanced oxidation processes for degrading pharmaceuticals in wastewater—a review," *catalysts*, vol. 14, no. 3, p. 189, 2024. [Online]. Available: <https://doi.org/10.3390/catal14030189>
- [18] V. Mishra, V. Mahajan, and J. Joshi, "wet air oxidation," *industrial engineering chemistry research*, vol. 34, no. 1, pp. 2–48, 1995. [Online]. Available: <https://doi.org/10.1021/ie00040a001>
- [19] J. Bai, Y. Liu, J. li, b. Zhou, Q. Zheng, and W. Cai, "A novel thin-layer photoelectrocatalytic (pec) reactor with double-faced titania nanotube arrays electrode for effective degradation of tetracycline," *Applied Catalysis B: Environmental*, vol. 98, no. 3-4, pp. 154–160, 2010. [Online]. Available: <https://doi.org/10.1016/j.apcatb.2010.05.024>
- [20] Z. Zhao, Z. Wu, X. Lin, F. Han, Z. Liang, L. Huang, and L. Niu, "A label-free pec aptasensor platform based on g-c₃n₄/bivo₄ heterojunction for tetracycline detection in food analysis," *food chemistry*, vol. 402, p. 134258, 2023. [Online]. Available: <https://doi.org/10.1016/j.foodchem.2022.134258>
- [21] P. Fernandez-Ibanez, S. McMichael, A. Cabanillas, S. Alkharabsheh, A. Moranchel, and J. Byrne, "New trends on photoelectrocatalysis (pec): nanomaterials, wastewater treatment and hydrogen generation," *Current Opinion in Chemical Engineering*, vol. 34, p. 100725, 2021. [Online]. Available: <https://doi.org/10.1016/j.coche.2021.100725>
- [22] X. Dong, D. Liu, X. Meng, and T. You, "Research progress on photoelectrochemical sensors for contamination analysis in agricultural fields," *Analytical sciences*, vol. 38, no. 3, pp. 459–481, 2022. [Online]. Available: <https://doi.org/10.2116/analsci.21SAR09>
- [23] S. Ye, Y. Chen, X. Yao, and J. Zhang, "Simultaneous removal of organic pollutants and heavy metals in wastewater by photoelectrocatalysis: a review," *Chemosphere*, vol. 273, p. 128503, 2021. [Online]. Available: <https://doi.org/10.1016/j.chemosphere.2020.128503>
- [24] Q. Dang, L. wang, J. Liu, D. wang, J. Chai, M. Wu, and L. Tang, "Recent progress of photoelectrocatalysis systems for wastewater treatment," *Journal of Water Process Engineering*, vol. 53, no. 9, p. 103609, 2023. [Online]. Available: <https://doi.org/10.1016/j.jwpe.2023.103609>
- [25] T. Ochiai and A. Fujishima, "Photoelectrochemical properties of tio₂ photocatalyst and its applications for environmental purification," *Journal of photochemistry and photobiology c: photochemistry reviews*, vol. 13, no. 4, pp. 247–262, 2012. [Online]. Available: <https://doi.org/10.1016/j.jphotochemrev.2012.07.001>
- [26] S. Mcmichael, P. Fernández-Ibáñez, and J. Byrne, "A review of photoelectrocatalytic reactors for water and wastewater treatment," *Water*, vol. 13, no. 9, p. 1198, 2021. [Online]. Available: <https://doi.org/10.3390/w13091198>
- [27] E. Zarei and R. Ojani, "Fundamentals and some applications of photoelectrocatalysis and effective factors on its efficiency: A review," *Journal of Solid State Electrochemistry*, vol. 21, no. 2, pp. 305–336, 2017. [Online]. Available: <https://doi.org/10.1007/s10008-016-3385-2>
- [28] J. Liu, H. Wu, J. Sun, S. Li, A. Hassani, and M. Zhou, "Non-tio₂-based photoanodes for photoelectrocatalytic wastewater treatment: electrode synthesis, evaluation, and characterization," *EES catalysis*, vol. 3, no. 5, pp. 921–942, 2025. [Online]. Available: <https://doi.org/10.1039/d5ey00068h>
- [29] A. Ali, S. Mohapatra, J. Van, and H. Spanjers, "bivo₄-based photoanodes for the photoelectrocatalytic removal of trace organic pollutants from water: a mini review on recent developments," *Current opinion in environmental science health*, vol. 45, p. 100615, 2025. [Online]. Available: <https://doi.org/10.1016/j.coesh.2025.100615>
- [30] M. Tayebi, Z. Masoumi, b. seo, c. Lim, H. Kim, and B. Lee, "Efficient and stable moo_x@ mo-bivo₄ photoanodes for photoelectrochemical water oxidation: optimization and understanding," *ACS applied energy materials*, vol. 5, no. 9, pp. 11568–11580, 2022. [Online]. Available: <https://doi.org/10.1021/acsaem.2c02066>
- [31] H. Yu, X. Sun, b. Zhao, W. Fan, W. Qin, M. Huo, and Y. Lu, "Enhanced photoelectrocatalytic degradation of tetracycline using a bifacial electrode of nickel-polyethylene glycol-pbo₂/ti/tio₂-ag₂o," *Journal of electroanalytical chemistry*, vol. 893, p. 115319, 2021. [Online]. Available: <https://doi.org/10.1016/j.jelechem.2021.115319>
- [32] S. Kahng and J. Kim, "Heterojunction photoanode of sno₂ and mo-doped bivo₄ for boosting photoelectrochemical performance and tetracycline hydrochloride degradation," *Chemosphere*, vol. 291, no. part 2, p. 132800, 2022. [Online]. Available: <https://doi.org/10.1016/j.chemosphere.2021.132800>
- [33] S. Yang, W. Choi, and H. Park, "tio₂ nanotube array photoelectrocatalyst and ni-sb-sno₂ electrocatalyst bifacial electrodes: a new type of bifunctional hybrid platform for water treatment," *ACS applied materials*

- interfaces*, vol. 7, no. 3, pp. 1907–1914, 2015. [Online]. Available: <https://doi.org/10.1021/am5076748>
- [34] J. Zhang, J. Luo, X. Zhao, K. wang, T. Xie, T. Xu, and M. Qiao, “Enhanced photoelectrocatalytic decomplexation of ni-edta and simultaneous recovery of metallic nickel via tio₂/ni-sb-sno₂ bifunctional photoanode and activated carbon fiber cathode,” *Journal of environmental sciences*, vol. 126, pp. 198–210, 2023. [Online]. Available: <https://doi.org/10.1016/j.jes.2022.05.023>
- [35] f. Yu, s. Hong, b. Guo, X. Ren, and X. Zhou, “tio₂ nanotubes array based ti/tio₂nts/sno₂-sb-bi/nato electrode for electrosynthesis of ozone water and application in wastewater treatment,” *Materials Science in Semiconductor Processing*, vol. 186, p. 109098, 2025. [Online]. Available: <https://doi.org/10.1016/j.mssp.2024.109098>
- [36] J. Mora-Gomez, M. Garcia-Gabaldon, E. Otega, M. Sanchez-Rivera, S. Mestre, and V. Pérez-herranz, “Evaluation of new ceramic electrodes based on sb-doped sno₂ for the removal of emerging compounds present in wastewater,” *Ceramics international*, vol. 44, no. 2, pp. 2216–2222, 2018. [Online]. Available: <https://doi.org/10.1016/j.ceramint.2017.10.178>
- [37] C. Domingo-Torner, M. García-Gabaldón, M. Martí-Calatayud, S. Mestre, and V. Pérez-Herranz, “Norfloxacin mineralization under light exposure using sb–sno₂ ceramic anodes coated with bifeo₃ photocatalyst,” *Chemosphere*, vol. 313, p. 137518, 2023. [Online]. Available: <https://doi.org/10.1016/j.chemosphere.2022.137518>
- [38] H. Uonis and A. Abbar, “Photoelectrocatalytic degradation of tetracycline by a novel gr/ni-sb-sno₂ photo-anode,” *South African Journal of Chemical Engineering*, vol. 55, pp. 24–39, 2026. [Online]. Available: <https://doi.org/10.1016/j.sajce.2025.10.004>
- [39] J. López-Peñalver, M. Sánchez-Polo, C. Gómez-Pacheco, and J. Rivera-Utrilla, “Photodegradation of tetracyclines in aqueous solution by using uv and uv/h₂o₂ oxidation processes,” *Journal of Chemical Technology and Biotechnology*, vol. 85, no. 10, pp. 1325–1333, 2010. [Online]. Available: <https://doi.org/10.1002/jctb.2435>
- [40] Y. Liu, X. Gan, B. Zhou, B. Xiong, J. Li, and e. a. Dong, C., “Photoelectrocatalytic degradation of tetracycline by highly effective tio₂ nanopore arrays electrode,” *Journal of hazardous materials*, vol. 171, no. 1–3, pp. 678–683, 2009. [Online]. Available: <https://doi.org/10.1016/j.jhazmat.2009.06.054>
- [41] F. Abd and A. Abbar, “Treatment of hospital wastewater by anodic oxidation using a new approach made by combining rotation with pulsed electric current on cu-sno₂-sb₂o₅ rotating cylinder anode,” *Heliyon*, vol. 11, no. 2, p. e42069, 2025. [Online]. Available: <https://doi.org/10.1016/j.heliyon.2025.e42069>
- [42] G. Asgari, A. Seid-mohammadi, A. Rahmani, R. Shokoohi, and H. Abdipour, “Concurrent elimination of arsenic and nitrate from aqueous environments through a novel nanocomposite: fe₃o₄-zif₈@ eggshell membrane matrix,” *Journal of molecular liquids*, vol. 411, no. 1, p. 125810, 2024. [Online]. Available: <https://doi.org/10.1016/j.molliq.2024.125810>
- [43] M. Zhou, Q. Dai, L. Lei, C. Ma, and D. Wang, “Long life modified lead dioxide anode for organic wastewater treatment: electrochemical characteristics and degradation mechanism,” *Environmental science technology*, vol. 39, no. 1, pp. 363–370, 2005. [Online]. Available: <https://doi.org/10.1021/es049313a>
- [44] Y. Sun, s. Cheng, L. li, Z. Yu, Z. Mao, and H. Huang, “Facile sealing treatment with stannous citrate complex to enhance performance of electrodeposited ti/sno₂-sb electrode,” *Chemosphere*, vol. 255, p. 126973, 2020. [Online]. Available: <https://doi.org/10.1016/j.chemosphere.2020.126973>
- [45] H. Nsaif, N. Majeed, and R. Salman, “Preparation of nano sno₂-sb₂o₃ composite electrode by cathodic deposition for the elimination of phenol by sonoelectrochemical oxidation,” *Polish Journal of Chemical Technology*, vol. 26, no. 3, p. 327, 2024. [Online]. Available: <https://doi.org/10.2478/pjct-2024-0026>
- [46] H. Nsaif and N. Majeed, “Modified graphite with tin oxide as a promising electrode for reduction of organic pollutants from wastewater by sonoelectrochemical oxidation,” *Ecological engineering environmental technology*, vol. 25, no. 1, pp. 307–320, 2024. [Online]. Available: <https://doi.org/10.12912/27197050/175437>
- [47] N. Entezami, M. Farhadian, A. Nazar, and S. Tangestaninejad, “Tetracycline removal from aqueous solution through photoelectrochemical oxidation process using bi₂o₃/zif-67@gp under visible light irradiation: effects of operational parameters, water matrix,” *Chemical Engineering and processing-process intensification*, vol. 188, no. 1, p. 109370, 2023. [Online]. Available: <https://doi.org/10.1016/j.cep.2023.109370>
- [48] G. Dinesh and R. Saranya, “Sonochemical facile synthesis of bismuth oxide nanoparticles using citrus lemon extract and its catalytic activity on azo dye degradation,” *Water, air, soil pollution*, vol. 235, p. 621, 2024. [Online]. Available: <https://doi.org/10.1007/s11270-024-07355-3>
- [49] M. Petrović, I. Slipper, M. Antonijević, g. Nikolić, J. Mitrović, D. Bojić, and A. Bojić, “Characterization of a bi₂o₃ coat based anode prepared by galvanostatic electrodeposition and its use for the electrochemical degradation of reactive orange 4,” *Journal of the Taiwan Institute of Chemical Engineers*, vol. 50, pp. 282–287, 2015. [Online]. Available: <https://doi.org/10.1016/j.jtice.2014.12.010>
- [50] A. Ahamed, P. Kumar, and M. Karthikeyan, “Wet chemical synthesis and characterization of nio nanoparticles,” *Int. j. nano. corr. sci. engg.*, vol. 2, no. 5, pp. 31–38, 2015.
- [51] H. Qiao, Z. Wei, H. Yang, L. Zhu, and X. Yan, “Preparation and characterization of nio nanoparticles by anodic arc plasma method,” *Journal of nanomaterials*, vol. 2009, no. 1, p. 795928, 2009. [Online]. Available: <https://doi.org/10.1155/2009/795928>
- [52] I. Shakir, S. Haider, P. Agboola, and N. Al-khali, “Fabrication of nio/sno₂ heterojunction based photocatalyst for efficient sunlight degradation of organic dyes,” *Journal of Taibah University for Science*, vol. 15, no. 1, pp. 656–665, 2021. [Online]. Available: <https://doi.org/10.1080/16583655.2021.1996135>
- [53] N. Srivastava and P. Srivastava, “Realizing nio nanocrystals from a simple chemical method,” *Bulletin of materials science*, vol. 33, pp. 653–656, 2010. [Online]. Available: <https://doi.org/10.1007/s12034-011-0142-0>
- [54] X. Li, D. Shao, H. Xu, W. Lv, and W. Yan, “Fabrication of a stable ti/tioxy/sb sno₂ anode for aniline degradation in different electrolytes,” *Chemical engineering Journal*, vol. 285, no. 1, pp. 1–10, 2016. [Online]. Available: <https://doi.org/10.1016/j.cej.2015.09.089>
- [55] L. Zhang, L. Xu, J. he, and J. Zhang, “Preparation of ti/sno₂-sb electrodes modified by carbon nanotube for anodic oxidation of dye wastewater and combination with nanofiltration,” *Electrochimica acta*, vol. 117, no. 1, pp. 192–201, 2014. [Online]. Available: <https://doi.org/10.1016/j.electacta.2013.11.117>
- [56] W. Zhao, J. Xing, D. Chen, Z. Bai, and Y. Xia, “Study on the performance of an improved ti/sno₂-sb 2 o 3/pbo 2 based on porous titanium substrate compared with planar titanium substrate,” *RSC Advances*, vol. 5, no. 34, pp. 26530–26539, 2015. [Online]. Available: <https://doi.org/10.1039/C4RA13492C>
- [57] T. Duan, Q. Wen, Y. Chen, Y. Zhou, and Y. Duan, “Enhancing electrocatalytic performance of sb-doped sno₂ electrode by compositing nitrogen-doped graphene nanosheets,” *Journal of hazardous materials*, vol. 280, pp. 304–314, 2014. [Online]. Available: <https://doi.org/10.1016/j.jhazmat.2014.08.018>
- [58] S. Yang, D. Kim, and H. Park, “Shift of the reactive species in the sb–sno₂-electrocatalyzed inactivation of e. coli and degradation of phenol: effects of nickel doping and electrolytes,” *Environmental science technology*, vol. 48, no. 5, pp. 2877–2884, 2014. [Online]. Available: <https://doi.org/10.1021/es404688z>
- [59] P. Alulema-Pullupaxi, P. Espinoza-Montero, C. Sigcha-Pallo, R. Vargas, L. Fernández, J. Peralta-Hernandez, and J. Paz, “Fundamentals and applications of photoelectrocatalysis as an efficient process to remove pollutants from water: a review,” *Chemosphere*, vol. 281, p. 130821, 2021. [Online]. Available: <https://doi.org/10.1016/j.chemosphere.2021.130821>
- [60] Y. Peng, H. Chen, and C. Huang, “The synergistic effect of photoelectrochemical (pec) reactions exemplified by concurrent perfluorooctanoic acid (pfoa) degradation and hydrogen generation over carbon and nitrogen codoped tio₂ nanotube arrays (c-n-ntas) photoelectrode,” *Applied Catalysis B: Environmental*, vol. 209, pp. 437–446, 2017. [Online]. Available: <https://doi.org/10.1016/j.apcatb.2017.02.084>
- [61] P. Kaur, Y. Park, M. Sillanpää, and M. Imteaz, “Synthesis of a novel sno₂/graphene-like carbon/tio₂ electrodes for the degradation of recalcitrant emergent pharmaceutical pollutants in a photo-electrocatalytic system,” *Journal of cleaner production*, vol. 313, p. 127915, 2021. [Online]. Available: <https://doi.org/10.1016/j.jclepro.2021.127915>
- [62] A. Ahdour, N. Douihi, A. Taoufyq, L. Aneflous, b. Bakiz, and A. Benlhamchemi, “Electrocatalytic and photoelectrocatalytic degradation of tetracycline using bahpo₄/ssa photoanode: insights from bbd-rsm and ccd-rsm experimental designs,” *Surfaces and interfaces*, vol. 58, p. 105874, 2025. [Online]. Available: <https://doi.org/10.1016/j.surf.2025.105874>

- [63] B. Orimolade, B. Zwane, B. Koiki, M. Rivallin, M. Bechelany, N. Mabuba, and O. Arotiba, "Coupling cathodic electro-fenton with anodic photo-electrochemical oxidation: a feasibility study on the mineralization of paracetamol," *Journal of Environmental Chemical Engineering*, vol. 8, no. 5, p. 104394, 2020. [Online]. Available: <https://doi.org/10.1016/j.jece.2020.104394>
- [64] E. Umukoro, N. Kumar, J. Ngila, and O. Arotiba, "Expanded graphite supported p-n mos2-sno2 heterojunction nanocomposite electrode for enhanced photo-electrocatalytic degradation of a pharmaceutical pollutant," *Journal of electroanalytical chemistry*, vol. 827, pp. 193–203, 2018. [Online]. Available: <https://doi.org/10.1016/j.jelechem.2018.09.027>
- [65] O. Ama, N. Mabuba, and O. Arotiba, "Synthesis, characterization, and application of exfoliated graphite/zirconium nanocomposite electrode for the photoelectrochemical degradation of organic dye in water," *Electrocatalysis*, vol. 6, pp. 390–397, 2015. [Online]. Available: <https://doi.org/10.1007/s12678-015-0258-x>
- [66] H. Rajput, E. Kwon, S. Younis, S. Weon, T. Jeon, W. Choi, and K. Kim, "Photoelectrocatalysis as a high-efficiency platform for pulping wastewater treatment and energy production," *Chemical engineering Journal*, vol. 412, p. 128612, 2021. [Online]. Available: <https://doi.org/10.1016/j.cej.2021.128612>
- [67] M. Pirsahab, H. Hoseini, and V. Abtin, "Photoelectrocatalytic degradation of humic acid and disinfection over nitio2-ni/ac-ptfe electrode under natural sunlight irradiation: modeling, optimization and reaction pathway," *Journal of the Taiwan Institute of Chemical Engineers*, vol. 118, pp. 204–214, 2021. [Online]. Available: <https://doi.org/10.1016/j.jtice.2020.12.023>
- [68] L. Tang, J. Wang, G. Zeng, Y. Liu, Y. Deng, Y. Zhou, and Z. Guo, "Enhanced photocatalytic degradation of norfloxacin in aqueous bi2wo6 dispersions containing nonionic surfactant under visible light irradiation," *Journal of hazardous materials*, vol. 306, no. 10, pp. 295–304, 2016. [Online]. Available: <https://doi.org/10.1016/j.jhazmat.2015.12.044>
- [69] E. Kusmierek, "Semiconductor electrode materials applied in photoelectrocatalytic wastewater treatment—an overview," *Catalysts*, vol. 10, no. 4, p. 439, 2020. [Online]. Available: <https://doi.org/10.3390/catal10040439>
- [70] A. Tayyebi, T. Soltani, and B. Lee, "Effect of ph on photocatalytic and photoelectrochemical (pec) properties of monoclinic bismuth vanadate," *Journal of Colloid and Interface Science*, vol. 534, pp. 37–46, 2019. [Online]. Available: <https://doi.org/10.1016/j.jcis.2018.08.095>
- [71] X. Zhou, Y. Zheng, J. Zhou, and S. Zhou, "Degradation kinetics of photoelectrocatalysis on landfill leachate using codoped tio2/ti photoelectrodes," *Journal of nanomaterials*, vol. 2015, no. 1, p. 810579, 2015. [Online]. Available: <https://doi.org/10.1155/2015/810579>
- [72] H. Znad, K. Abbas, S. Hena, and M. Awwal, "Synthesis a novel multilamellar mesoporous tio2/zsm-5 for photo-catalytic degradation of methyl orange dye in aqueous media," *Journal of Environmental Chemical Engineering*, vol. 6, no. 1, pp. 218–227, 2018. [Online]. Available: <https://doi.org/10.1016/j.jece.2017.11.077>
- [73] W. Xie, Y. Shi, Y. Wang, Y. Zheng, H. Liu, Q. Hu, and Z. Guo, "Electrospun iron/cobalt alloy nanoparticles on carbon nanofibers towards exhaustive electrocatalytic degradation of tetracycline in wastewater," *Chemical engineering Journal*, vol. 405, no. 14, p. 126585, 2021. [Online]. Available: <https://doi.org/10.1016/j.cej.2020.126585>
- [74] H. Cho, H. Seo, H. Joo, J. Kim, and J. Yoon, "Performance evaluation of rotating photoelectrocatalytic reactor for enhanced degradation of methylene blue," *Korean Journal of Chemical Engineering*, vol. 34, no. 10, pp. 2780–2786, 2017. [Online]. Available: <https://doi.org/10.1007/s11814-017-0198-7>
- [75] K. Li, C. Yang, Y. Wang, J. Jia, Y. Xu, and Y. He, "A high-efficient rotating disk photoelectrocatalytic (pec) reactor with macro light harvesting pyramid-surface electrode," *Aiche Journal*, vol. 58, no. 8, pp. 2448–2455, 2012. [Online]. Available: <https://doi.org/10.1002/aic.12755>
- [76] Y. Xu, Y. he, X. Cao, d. Zhong, and J. Jia, "tio2/ti rotating disk photoelectrocatalytic (pec) reactor: a combination of highly effective thin-film pec and conventional pec processes on a single electrode," *Environmental science technology*, vol. 42, no. 7, pp. 2612–2617, 2008. [Online]. Available: <https://doi.org/10.1021/es702921h>
- [77] A. Das and L. Chen, "A review on electrochemical advanced oxidation treatment of dairy wastewater," *environments*, vol. 11, no. 6, p. 124, 2024. [Online]. Available: <https://doi.org/10.3390/environments11060124>
- [78] M. Collivignarelli, M. Carnevale miino, H. Arab, M. Bestetti, and S. Franz, "Efficiency and energy demand in polishing treatment of wastewater treatment plants effluents: photoelectrocatalysis vs. photocatalysis and photolysis," *Water*, vol. 13, no. 6, p. 821, 2021. [Online]. Available: <https://doi.org/10.3390/w13060821>
- [79] X. Liang, S. Yu, B. Meng, X. Wang, C. Yang, C. Shi, and J. Ding, "Advanced tio 2-based photoelectrocatalysis: material modifications, charge dynamics, and environmental-energy applications," *Catalysts*, vol. 15, no. 6, p. 542, 2025. [Online]. Available: <https://doi.org/10.3390/catal15060542>
- [80] E. Brillas and C. Martínez-huitle, "Decontamination of wastewaters containing synthetic organic dyes by electrochemical methods. an updated review," *Applied Catalysis B: Environmental*, vol. 166–167, pp. 603–643, 2015. [Online]. Available: <https://doi.org/10.1016/j.apcatb.2014.11.016>
- [81] P. Nidheesh, M. Zhou, and M. Oturan, "An overview on the removal of synthetic dyes from water by electrochemical advanced oxidation processes," *Chemosphere*, vol. 197, no. 3, pp. 210–227, 2018. [Online]. Available: <https://doi.org/10.1016/j.chemosphere.2017.12.195>
- [82] C. Sigcha Pallo, "Estudio de la degradación de diclofenaco en medio acuoso mediante fotoelectrocatalisis empleando un fotoánodo de diamante dopado con boro (bdd) modificado con dióxido de titanio (tio2) (bachelor's thesis, quito)," 2020.
- [83] M. Carreño-lizcano, A. Gualdrón-reyes, V. Rodríguez-González, J. Pedraza-Avella, and M. Niño-Gómez, "Photoelectrocatalytic phenol oxidation employing nitrogen doped tio2-rgo films as photoanodes," *Catalysis today*, vol. 341, pp. 96–103, 2020. [Online]. Available: <https://doi.org/10.1016/j.cattod.2019.02.006>
- [84] B. Orimolade, b. Koiki, G. Peleyeju, and O. Arotiba, "Visible light driven photoelectrocatalysis on a fto/bivo4/bioi anode for water treatment involving emerging pharmaceutical pollutants," *Electrochimica acta*, vol. 307, pp. 285–292, 2019. [Online]. Available: <https://doi.org/10.1016/j.electacta.2019.03.217>
- [85] A. Huda, P. Suman, L. Torquato, B. Silva, C. Handoko, F. Gulo, and M. Orlandi, "Visible light-driven photoelectrocatalytic degradation of acid yellow 17 using sn3o4 flower-like thin films supported on ti substrate (sn3o4/tio2/ti)," *Journal of photochemistry and photobiology a: chemistry*, vol. 376, pp. 196–205, 2019. [Online]. Available: <https://doi.org/10.1016/j.jphotochem.2019.01.039>
- [86] J. De Brito, G. Bessegato, T. Viana, D. de Oliveira, C. Martínez-huitle, and M. Zanoni, "Combination of photoelectrocatalysis and ozonation as a good strategy for organics oxidation and decreased toxicity in oil-produced water," *Journal of the Electrochemical Society*, vol. 166, no. 5, p. h3231, 2019. [Online]. Available: <https://doi.org/10.1149/2.0331905jes>
- [87] G. Li, T. An, J. Chen, G. Sheng, J. Fu, F. Chen, and H. Zhao, "Photoelectrocatalytic decontamination of oilfield produced wastewater containing refractory organic pollutants in the presence of high concentration of chloride ions," *Journal of Hazardous Materials*, vol. 138, no. 2, pp. 392–400, 2006. [Online]. Available: <https://doi.org/10.1016/j.jhazmat.2006.05.083>
- [88] L. Cheng, T. Jiang, K. Yan, J. Gong, and J. Zhang, "A dual-cathode photoelectrocatalysis-electroenzymatic catalysis system by coupling bivo4 photoanode with hemin/cu and carbon cloth cathodes for degradation of tetracycline," *Electrochimica Acta*, vol. 298, no. 1, pp. 561–569, 2019. [Online]. Available: <https://doi.org/10.1016/j.electacta.2018.12.086>

How to cite this article:

Heba F. Uonis and Ali H. Abbar, (2026). 'Treatment of petroleum refinery wastewater by photo-anodic oxidation process with Gr/Bi-Ni-Sb-SnO2 rotating photo-anode: Performance and kinetic study', *Al-Qadisiyah Journal for Engineering Sciences*, 19(1), pp. 049-058. <https://doi.org/10.30772/qjes.2025.165011.1742>